

# Numerical Investigation Of Throttle Valve Flow Characteristics For Internal Combustion Engines

**Mustapha Bordjane**

Université des Sciences et de la Technologie  
Mohamed Boudiaf d'Oran, IGCMO-LMA  
Oran, Algeria

**David Chalet**

Ecole Centrale de Nantes  
LHEEA Lab. (ECN/CNRS)  
Nantes, France

**Abstract—** Gas exchange processes of internal combustion engines have an important effect on engine performances, emissions of pollutants and noise. To control the engine output torque by the intake airflow restriction, a throttle valve must be installed between the air cleaner and the intake manifold. Due to the complex nature of this unit geometry and the resulting flow field, a 3D flow model would be indispensable to predict precisely the relative flow behavior. Actually, CFD codes and models are used in the design starting point. One of the major advantages of numerical investigation of turbulent flows is the capability to change easily the geometry, dynamic and thermodynamic parameters for the problem treated. Hence, we can study the effect of these parameters avoiding repetition of experimentation, which is usually time consuming and costly. However, the experimental measures will stay and forever the only way to validate the numeral calculations. To develop this subject, numerical investigation and analytical analysis have been proposed in this paper. First, we have used existing mathematical model (Barré de Saint Venant model), to check if it can be applied to study this kind of flow. Simultaneously, 3D investigation was carried out to study the mean and turbulent flow characteristics. Then, results obtained from the simulation model are compared with those obtained analytically and experimentally. Acceptable agreement is noticed from the use of the 3D viscous model in conjunction with the Barré de Saint Venant model. Future recommendations for modeling improvements were suggested in the end of this paper to correct the quasi-steady (or BSV) model.

**Keywords—** internal combustion engines, throttle valve, CFD simulation, modeling methods, fluid flow, turbulence models

## I. INTRODUCTION

A major goal of engine manufacturers is to minimize specific fuel consumption and emission from engines. A major disadvantage of conventional spark ignition (SI) engines results from the energy losses

during inhaling of atmospheric gases during the suction stroke and expelling of exhaust gases to the atmosphere during the exhaust stroke. The pumping losses depend on the opening and closing positions of the throttle valve. The losses are high when the throttle valve tends to close and are low at Wide-Open-Throttle (WOT). Thus, the pumping losses are inversely proportional with the engine load [1].

Gas exchange systems of internal combustion engines play a major role and have an important effect on engine performances, emissions of pollutants and noise. The use of high technology research and design tools allowed the improvement of these accomplishments within low cost and limited time. One of these tools is CFD. CFD is helping automotive engineers to better understand the physical flow processes, and in turn to design improved vehicle.

Today, the massive power of modern CFD is being applied by automotive engineers to study all details aspects of internal combustion engine flow fields, including combustion, turbulence, and coupling with the manifold and exhaust pipes [2]. The indicated power of an internal combustion engine at a given speed is proportional to the mass of air contained in the cylinder. Thus, including the maximum air mass at Wide-Open-Throttle (WOT) or fuel load and retaining that mass within the cylinder is one of the major goals of the gas exchange processes [3]. The function of the throttle body is to control the engine output torque by the intake airflow restriction.

From literature, there are two main types of computer model for engine flow: zero-dimensional or phenomenological models, which are thermodynamic in nature with time as the only independent variable, and multi-dimensional models, which resolve the variations of mass, momentum and energy in all three dimensions and time [4-6]. The third type is the quasi-steady compressible flow model. Junctions representing valves and orifices (throttle valve) are described by quasi-steady compressible flow models [7].

From a comparison between experimental results and one-dimensional simulation using gas dynamic equations it appears that the pressure drop around the

throttle valve seems to be correctly evaluated only if the difference between the initial inner pressure and the atmospheric pressure remains small. This corresponds also to a small flow velocity. Consequently, Chalet *et al* [8] show the deficiency of the model based on Winterbone approach (the use of the coefficient that depends on the opening rate of the throttle value) to correct the errors between real state and modeling (e.g. one-dimensional gas dynamic equations). So, CFD code will be used as a numerical test bench in which more information about fluid flow characteristics (density, velocity, etc...) can be known. These characteristics are not available when conducting experimental study [8]. In this study, numerical investigation using Ansys.CFX.CFD code, isentropic compressible fluid flow model (Barré de Saint Venant model) and experimental data [9] are used to evaluate the fluid flow through the throttle valve of internal combustion engine.

## II. PHYSICAL MODEL DESCRIPTION

The throttle body is the element which allows the regulation or control of the amount of ambient air inflowing in the manifold of internal combustion engine. The throttle valve admits air flow from one end of the manifold, while the cylinder draws air out from the other end. Air passes through a filter before being regulated by a throttle valve. By modeling air induction, we can come into the assumption that the engine is a volumetric pump [10]. For the conventional engine control systems, throttle angle is directly controlled by the driver using a mechanical connection from accelerator pedal to the engine throttle.



Fig. 1. Typical throttle body used in Internal Combustion Engine

For an internal combustion engine, the throttle body consists of cylindrical bore crossed by a shaft on which is mounted an elliptical throttle butterfly plate. Fig. 1 shows the typical throttle body used in internal combustion engines. To prevent the butterfly bending in the throttle bore, the closed plate angle is not zero; it must be between (5° and 15°). The pumping action of the piston will draw air from the manifold into the cylinder. The reduction in pressure will in turn, draw air into the manifold from the environment. The purpose of the throttle valve is to regulate the flow of this air. A throttle plate of conventional design (such as the one

in Fig.1) creates a three-dimensional flow field, which requires a 3D CFD investigation.

Geometric description of typical devices used in this study is presented in Fig. 2.

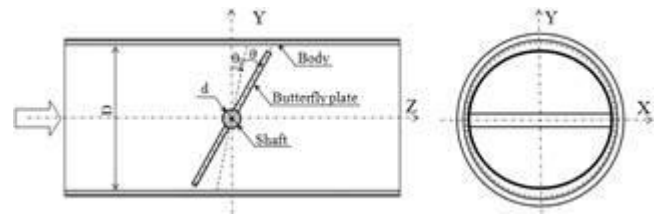


Fig. 2. Geometric description of the throttle body

## III. 3D-CFD MODEL

The geometry of the throttle body opening changes with varying throttle angle. To predict accurately the airflow through the throttle body, a three-dimensional model would be suitable due to the complex geometry. The computational requirements of such a model would be prohibitive [11]. The physical domain of the throttle body used in this study is composed of a system of two pipes (200 mm length and 60 mm inner diameter for each one), the throttle valve (bore diameter  $D=60$  mm) is positioned between the later pipes. The valve shaft diameter is 10 mm and its thickness is 3mm. In order to reduce the computational times, just a half of the geometry is used as numerical domain. Sixteen values of the opening valve angles (from the Closed In Bore,  $\theta_{CIB}=7^\circ$ ) are chosen to study numerically this engine singularity,  $\theta = (1, 2, 3, 4, 6, 8, 10, 15, 20, 25, 40, 50, 60, 70, 80$  and  $90)$  degrees. Numerical domain creation and mesh generation are realized using ICEM of Ansys.CFX. Fig.3 shows the configuration created with mesh. Simulations were performed using unstructured mesh (tetrahedral elements) with density varying from  $8 \cdot 10^5$  to  $15 \cdot 10^5$  cells.



Fig. 3. Numerical domain with mesh

Basically, it is necessary to discretize the governing equations to form a set of algebraic relationships, which can then be solved on a digital computer. The governing equations define the propagation of information through the fluid in the manifolds as pressure waves, which has a major effect on engine performance [12-13].

Multi-dimensional techniques for viscous flows are considerably more sophisticated than the 0D or 1D model [14]. The most complete mathematical description of fluids flow are the Navier-stokes equations (including continuity and energy) in 3D, supplemented by empirical laws relating the dependence of viscosity and thermal conductivity to the flow variables and by thermodynamic state relationships [14]. Time-averaging operation on the Navier-stokes momentum equations result in the Reynolds averaged Navier-stokes equations. A turbulence model is necessary: from a physical point of view it is an attempt to mimic physical information on the sub-grid scale turbulence which is lost by the temporal averaging of the momentum equations. From a mathematical point of view it is a mean of closing the set of Reynolds Navier-Stokes equations (providing additional relationships to make the number of equations equal the number of unknown). The (k-ε) approach of Launder and Spalding [14] is based on the assumption that the turbulent viscosity is isotropic. Two equations are to be solved for each computational cell; one for kinetic energy (k) and one for its rate of dissipation (ε). This model have been widely applied for simulating engine flows, being used extensively to model mixture preparation and flow through valves into engine cylinders and ensuing combustion. Flows through catalytic converters and other isolated manifold components have been simulated using the (k-ε) approach. While multi-dimensional calculations including turbulence models are now used routinely in the engine design, their use in intake and exhaust systems has largely been restricted to examining the local flow structures in isolated regions of manifolds where the flow is complex and separated (cylinders-port, assemblies, pressure loss junctions...etc.) [14].

Equations used to evaluate the steady state gas flow in manifolds of internal combustion engines are derived in several forms; in this study, the system of equations for steady state fluid flow is given by the famous equations of motion, which bears the names of Navier and Stokes.

A. Continuity equation

$$\frac{\partial \rho}{\partial t} + \frac{\partial}{\partial x_j}(\rho U_j) = 0 \quad (j=1, 2, 3) \quad (1)$$

B. Reynolds averaged momentum equations

$$\frac{\partial \rho U_i}{\partial t} + \frac{\partial}{\partial x_j}(\rho U_i U_j) = -\frac{\partial p}{\partial x_i} + \frac{\partial}{\partial x_j} \left[ \mu_{eff} \left( \frac{\partial U_i}{\partial x_j} + \frac{\partial U_j}{\partial x_i} \right) \right] \quad (2)$$

The time derivative ( $\partial/\partial t$ ) was kept in the equations just for not losing the generality aspect, but all calculations presented in this work, concern only steady solutions.  $\mu_{eff}$ , is the effective viscosity accounting for turbulence and  $p'$  is the modified pressure ( $p'=p+(2/3).\rho k$ ).

The purpose of turbulence model is practical; it is numerical prevision of turbulent flow to provide an

approximate description. The qualities wanted from turbulence model are: large application field, precision, simplicity and reduction of calculation time.

The k-ε model used here is based on the eddy viscosity concept; the effective viscosity is expressed by ( $\mu_{eff}=\mu+\mu_t$ ), where  $\mu_t$  is the turbulence viscosity, which is linked to the turbulence kinetic energy and dissipation rate via the relation:

$$\mu_t = C_\mu \cdot \rho \frac{k^2}{\varepsilon} \quad (3)$$

So, two new variables are introduced by this hypothesis in the system of equations (k and ε),  $C_\mu$  is a model constant. The values of k and ε come directly from the differential transport equations for the turbulence kinetic energy and the turbulence dissipation rate.

$$\frac{\partial(\rho k)}{\partial t} + \frac{\partial}{\partial x_j}(\rho U_j k) = \frac{\partial}{\partial x_j} \left[ \left( \mu + \frac{\mu_t}{\sigma_k} \right) \frac{\partial k}{\partial x_j} \right] + P_k - \rho \varepsilon \quad (4)$$

$$\frac{\partial(\rho \varepsilon)}{\partial t} + \frac{\partial}{\partial x_j}(\rho U_j \varepsilon) = \frac{\partial}{\partial x_j} \left[ \left( \mu + \frac{\mu_t}{\sigma_\varepsilon} \right) \frac{\partial \varepsilon}{\partial x_j} \right] + \frac{\varepsilon}{k} (C_{\varepsilon 1} P_k - C_{\varepsilon 2} \rho \varepsilon) \quad (5)$$

Where:  $C_{\varepsilon 1}$ ,  $C_{\varepsilon 2}$ ,  $\sigma_k$  and  $\sigma_\varepsilon$  are the model constants cited in Table 1.  $P_k$  is the turbulence production due to viscous forces which is modeled (6).

$$P_k = \mu_t \left( \frac{\partial U_i}{\partial x_j} + \frac{\partial U_j}{\partial x_i} \right) \frac{\partial U_i}{\partial x_j} - \frac{2}{3} \frac{\partial U_k}{\partial x_k} \left( 3\mu_t \frac{\partial U_k}{\partial x_k} + \rho k \right) \quad (6)$$

TABLE I. K-ε MODEL CONSTANTS

Symbols	$C_\mu$	$C_{\varepsilon 1}$	$C_{\varepsilon 2}$	$\sigma_k$	$\sigma_\varepsilon$
Values	0.09	1.44	1.92	1.00	1.3

C. Initial and boundary conditions

For the numerical solution, the simulation type is steady state. The initial conditions of the fluid domain were defined as: the fluid is considered to be air ideal gas at the initial temperature ( $T_{init}=298$  K), the imposed initial pressure is ( $P_{init}=0.7$  bar) to create the depression necessary for the fluid to flow through the throttle valve from the inlet boundary at pressure ( $P_{spec}=1.0$  bar)

Specifications of boundary conditions for the calculations are illustrated in Fig. 4.

At the inlet, the flow is subsonic, the relative pressure prescribed is ( $P_{spec}=1.0$  bar). The turbulence intensity at the core of a fully developed duct flow can be estimated from the following formula derived from an empirical correlation for pipe flows [15]:

$$I = \sqrt{u'} / U = 0.16. Re^{-1/8}; \quad (Re = U. D / \nu) \quad (7)$$

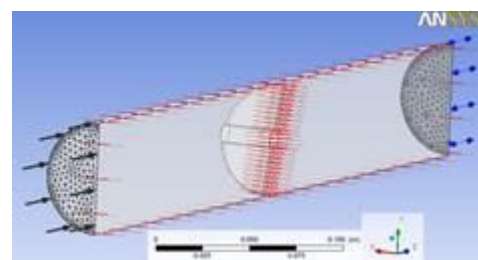


Fig. 4. Numerical domain with mesh

For internal flows, the turbulence intensity at the inlets is totally dependent on the upstream history of the flow. So, in the absence of any information's about the inlet turbulence, the intensity of turbulence is defined as:  $I=5\%$  and the viscosity ratio is  $\mu_v/\mu=10$ . Then,  $k$  and  $\varepsilon$  can be calculated using [16]:

$$k = \frac{3}{2} (I U)^2; \varepsilon = k^{3/2} / 0.3D \quad (8)$$

Where,  $D=0.06m$ .

The boundary type of the outlet is opening, this condition can be specified with a relative pressure value ( $P_{spec}=0.7bar$ ), the value is interpreted as: relative total pressure for inflow and relative static pressure for outflow. The symmetry plane boundary condition imposes constraints which mirror the flow in either side of it so, the normal velocity component at the symmetry plane boundary is set to be zero:  $V_n=0$ , and the scalar variable gradients normal to the boundary are also set to be zero:  $(\partial\phi/\partial n)=0$ .

The pipe is defined as an adiabatic wall which allows, no heat transfer across the wall boundary ( $q_w=0$ ) and no-slip boundary condition is imposed for the stationary solid wall so,  $U_w=0$ .

In the  $k-\varepsilon$  model, the  $k$  equation was solved in the whole domain including the wall-adjacent cells. The boundary condition for  $k$  imposed at the wall is given by  $(\partial k/\partial n=0)$ , where  $n$  is the local coordinate normal to the wall.

The production of kinetic energy  $P_k$  and its dissipation rate  $\varepsilon$ , at the wall-adjacent cells, are computed on the basis of the local equilibrium hypothesis. Under this assumption, the production of  $k$  and its dissipation rate are assumed to be equal in the wall-adjacent control volume. The wall-function approach [17] is used to provide near-wall boundary conditions for the mean flow and turbulence transport equations

#### IV. ISENTROPIC COMPRESSIBLE FLOW MODEL (BARRE DE SAINT VENANT MODEL)

The throttle body is not truly a one-dimensional orifice so; to imitate this kind of flow by the use of 1D model, other characteristics as 3D effects must be embodied in the discharge coefficient ( $C_D$ ). The throttle body equations consist of the valve equation and the air mass flow rate equations respectively. In the air admission model, one-dimensional isentropic analysis and ideal gas state equation were used to calculate admitted air mass and intake manifold pressure. Once the upstream stagnation pressure and temperature are established, the flow through the throttle body is a function of two independent parameters: the throttle angle and the pressure ratio across the throttle body [18]. Many engine control systems need to estimate throttle air mass flow ( $\dot{m}$ ) with throttle angle ( $\theta$ ) and either an intake manifold pressure ( $P_m$ ) or manifold vacuum measurement. For any given throttle, physics

and dimensional analysis also require upstream pressure ( $P_0$ ) and temperature ( $T_0$ ) measurements or estimates to arrive at mass flow [9].

Taylor [19] states a standard formula for compressible gas mass flow through a general passage. These functions were derived subject to the following simplifying assumptions:

- The flowing fluid is gas with constant specific heats obeying the ideal gas law ( $PV=nRT$ );
- An adiabatic thermodynamic process (no heat added or lost, gas in equilibrium at every stage);
- An isentropic process, also, we note that since the velocity distribution is uniform, the streamlines are parallel and thus a vena contracta (recirculation zone) would never form. This of course is contrary to observation;
- Inviscid gas (no shear stress, no friction between gas and conduit, implying a uniform velocity distribution across the conduit);
- Pressures and temperatures upstream and downstream are measured where gas kinetic energy is negligible.

Habitually, for a compressible fluid flow, the mass flow rates through the throttle valve can be calculated from the standard orifice equations.

Considering the case of pressure ratios across the throttle valve where they varied between the ambient (upstream) pressure  $P_0$  and the intake manifold (downstream) pressure  $P_m$  and for which the critical ratio is given by ( $P_m/P_0=0.528$ ,  $\gamma=1.4$ ).

For pressure ratios greater than the critical one (non-choked flow):

$$\frac{P_m}{P_0} \geq \left(\frac{2}{\gamma+1}\right)^{\gamma/(\gamma-1)} \quad (9)$$

The mass flow rate is given by:

$$\dot{m} = C_D \cdot A(\theta) \cdot \frac{P_0}{\sqrt{RT_0}} \cdot \left(\frac{P_m}{P_0}\right)^{1/\gamma} \cdot \sqrt{\left\{\frac{2\gamma}{\gamma-1} \left[1 - \left(\frac{P_m}{P_0}\right)^{(\gamma-1)/\gamma}\right]\right\}} \quad (10)$$

For pressure ratios less than the critical one (choked flow):

$$\frac{P_m}{P_0} < \left(\frac{2}{\gamma+1}\right)^{\gamma/(\gamma-1)} \quad (11)$$

The mass flow rate depends explicitly upon the pressure ratio and is given by:

$$\dot{m} = C_D \cdot A(\theta) \cdot \frac{P_0}{\sqrt{RT_0}} \cdot \sqrt{\gamma} \left(\frac{2}{\gamma+1}\right)^{(\gamma+1)/[2(\gamma-1)]} \quad (12)$$

Where;  $\gamma$  is the specific heat ratio,  $\dot{m}$  is the air mass flow rate,  $C_D$  is the discharge coefficient,  $A(\theta)$  is the passage flow area,  $R$  is the gas constant of air and  $T_0$  is the ambient temperature (upstream temperature) [18]. Many previous investigations have modeled the throttle body using the theory of one-dimensional isentropic compressible flow across an orifice modified by an empirically derived discharge coefficient,  $C_D$  [20].

The capacity to calculate  $C_D$  depends upon the proper characterization of the flow area profile as a function of throttle angle. Consequently, and for convenience, the flow area and the discharge coefficient were combining into a single effective area term [21],  $A_e$ :

$$A_e = C_D \cdot A(\theta) \quad (13)$$

From the mass flow rate (experimental or numerical) data,  $A_e$  was calculated using the following equations [21]:

For non-choked flow:

$$A_e = \frac{\dot{m}}{\frac{P_0}{\sqrt{RT_0}} \left(\frac{P_m}{P_0}\right)^{1/\gamma} \sqrt{\left\{ \frac{2\gamma}{\gamma-1} \left[ 1 - \left(\frac{P_m}{P_0}\right)^{(\gamma-1)/\gamma} \right] \right\}}} \quad (14)$$

For choked flow:

$$A_e = \frac{\dot{m}}{\frac{P_0}{\sqrt{RT_0}} \sqrt{\gamma} \left(\frac{2}{\gamma+1}\right)^{(\gamma+1)/[2(\gamma-1)]}} \quad (15)$$

Conventionally, drivers use the throttle to regulate engine power, through a non-linear but monotone increasing relation between throttle angle and area. Two equations usually used to calculate the throttle-effective area, Harington *et al* [22] proposed a formula (16) (with the use of Fig. 2) which gives the same results as that of Moskwa [11].

$$A(\theta) = \frac{\pi D^2}{4} \left(1 - \frac{\cos\theta}{\cos\theta_0}\right) + \frac{d}{2\cos\theta} \left(D^2 \cos^2\theta - d^2 \cos^2\theta_0\right)^{1/2} + \frac{D^2 \cos\theta}{2\cos\theta_0} \arcsin\left(\frac{a \cos\theta_0}{\cos\theta}\right) - \frac{d}{2} \sqrt{D^2 - d^2} + \frac{D^2}{2} \arcsin(a) \quad (16)$$

Where ( $a=d/D$ ),  $d$  is the throttle shaft diameter,  $D$  is the throttle bore diameter and  $\theta_0$  is the throttle plate angle when tightly closed against the throttle bore. Both models use the correction formula (17) for small angles.

$$\theta_0^* = 0.91\theta_0 - 2.59 \quad (17)$$

At a specified angle, the throttle-effective area reaches its maximum so, for  $\theta \geq \arccos\left(\frac{d}{D} \cos\theta_0\right) - \theta_0$ , we use the following equation [11]:

$$A(\theta) = \frac{D^2}{2} \arcsin\left[(1 - a^2)^{1/2}\right] - \frac{dD}{2} (1 - a^2)^{1/2} \quad (18)$$

## V. RESULTS AND DISCUSSION

The simulation and modeling methods for this sub-system of internal combustion engine consists, of the three dimensional CFD.CFX code which describes the mean and turbulent flow parameters and the quasi-steady compressible flow (or BSV) model. The flow area profile and the discharge coefficient are computed in the first stage using the numerical results of mass flow rate.

The simulation was also used to investigate the effect of throttle valve opening angle on the flow area and thus on mass flow rate, since, in the real case, increasing charge density to lead increasing volumetric

efficiency of the engine. From the scatter plot of valve open area  $A_{th}$  (Fig. 5) versus throttle angle data, it appears that the representative curve is sigmoid in nature and relatively smooth. This mathematical function, which having an "S" shape can be encountered in many applications. In our case, the scatter plot can be imitated by Gompertz curve. The late is used in modeling systems that saturate at large value of independent variable (throttle angle) or where growth is slower at the start and end of time period  $[0-90^\circ]$ .

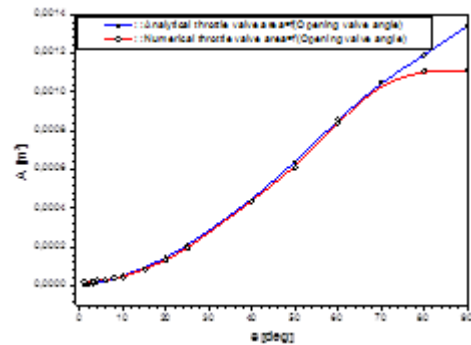


Fig. 5. Valve open area versus throttle angle ( $A=f(\theta)$ )

At small throttle angles, area variation versus throttle angle can't be adequately captured unless we include a leak area. Flow at small angles is dominated by this parameter, but the later effects decrease quite quickly with the increase of the valve opening. We see a small difference occurring only for large angles.

The cross-section area of gas reaches a maximal value at approximately (70°) of the opening angle of throttle plate (Fig. 5). Beyond this angle, the shaft of the throttle plate limits the passage of gases.

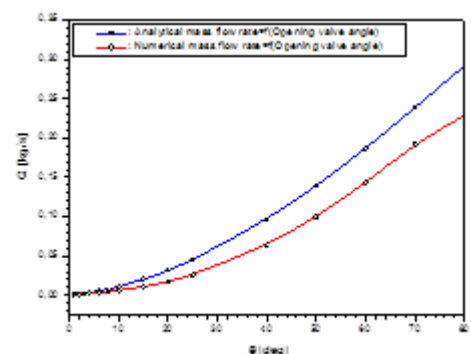


Fig. 6. Mass flow rate versus throttle angle ( $q=f(\theta)$ )

From Fig. 6, it is clear that the two models predict zero flow unless including a leak area. Generally, good agreement was observed between the two models. To understand why the mass flow rate evolves, we must return to the intake throttle body equation (10), as indicated previously, when  $(P_m/P_0)$  approaches 1, then  $\frac{\partial \dot{m}}{\partial (P_m/P_0)} \rightarrow \infty$ . Flow estimation using equation (10) will be very sensitive to small variations in pressure ratio measurements in operating regimes, such as low-speed WOT operation, where  $[(P_m/P_0) \rightarrow 1]$ . This is the useless practical defect or failing of using equation (10) to estimate the flow. We saw from this numerical

results that as opening valve angle increase,  $[(P_m/P_0) \rightarrow 1]$ , the mass flow becomes very sensitive to this ratio and consequently the estimation of discharge coefficient for opening angle near (WOT) is not successful (greater than one) using equation (10).

Another important fact is that, the mass flow rate through the throttle valve is expressed in function of the total pressure and total temperature at the upstream side, and the ratio between the downstream static pressure and the upstream total pressure. However, in real cases, the pressure measured on experimental apparatus, is the static one. Hence, taking into account the inlet velocity allowed the below corrections in the expressions of the mass flow rate.

For subsonic flow:

$$\dot{m} = A_e \cdot P_{up,stat} \cdot \sqrt{\frac{2\gamma}{R \cdot T_{up,stat}}} \cdot \frac{\frac{1}{\gamma-1} \left[ \left( \frac{P_{do}}{P_{up,stat}} \right)^{\frac{2}{\gamma}} - \left( \frac{P_{do}}{P_{up,stat}} \right)^{\frac{\gamma+1}{\gamma}} \right]}{1 - \left( \frac{P_{do}}{P_{up,stat}} \right)^{\frac{2}{\gamma}} \cdot \left( \frac{A_{th}}{A_{bore}} \right)^2} \quad (19)$$

For sonic flow:

$$\dot{m} = A_e \cdot P_{up,stat} \cdot \sqrt{\frac{2\gamma}{R \cdot T_{up,stat}}} \cdot \frac{\frac{1}{\gamma+1} \left( \frac{2}{\gamma+1} \right)^{\frac{2}{\gamma-1}}}{1 - \left( \frac{2}{\gamma+1} \right)^{\frac{2}{\gamma-1}} \cdot \left( \frac{A_{th}}{A_{bore}} \right)^2} \quad (20)$$

Or in CFD calculations, we use directly the total pressure and total temperature given by the inlet conditions:

$$P_{tot} = P_{stat} + P_{dyn} = P_{up,stat} + \rho_{up} \cdot \frac{U_{up}^2}{2} \quad (21)$$

$$T_{tot} = T_{stat} + \frac{U_{up}^2}{2 \cdot c_p} \quad (22)$$

These notions result from the application of the first principle of thermodynamics that permit to evaluate the variation of the system kinetic energy, which is equal to the enthalpy variation. In this situation, the hypothesis of no thermal exchange or adiabatic transformation and where, the upstream pressure ( $P_{up}$ ) is greater than the downstream pressure ( $P_{do}$ ) are considered.

Several flow characteristics and flow patterns can be prospected graphically by the use of CFD.CFX software. The results reproduce the nature of the flow, quantitatively and qualitatively, in direction and magnitude from the ambient environment to the manifold receptacle.

At small opening angles, it is observed from the streamlines and pressure contours (Fig. 7), the generation of vortices that move in the downward direction behind the throttle valve because of the high disturbance of the flow. The wake region containing the vortices is created at the downstream of the throttle plate and it is characterized by lower pressure. This wake region decays by increasing the throttle-opening angle and becomes relative to the throttle shaft (Fig. 8).

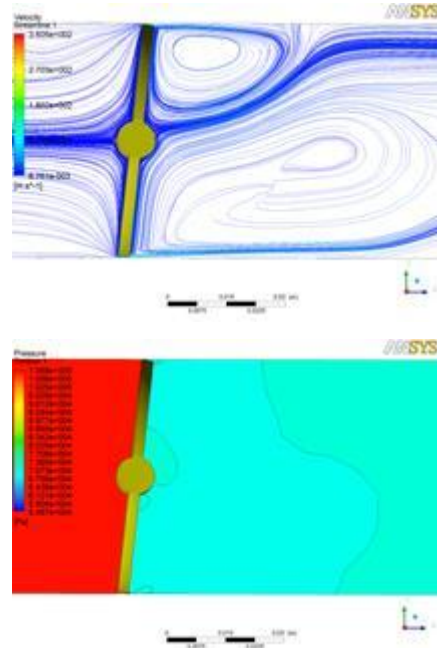


Fig. 7. Streamlines and pressure contours at  $(\theta=3^\circ)$

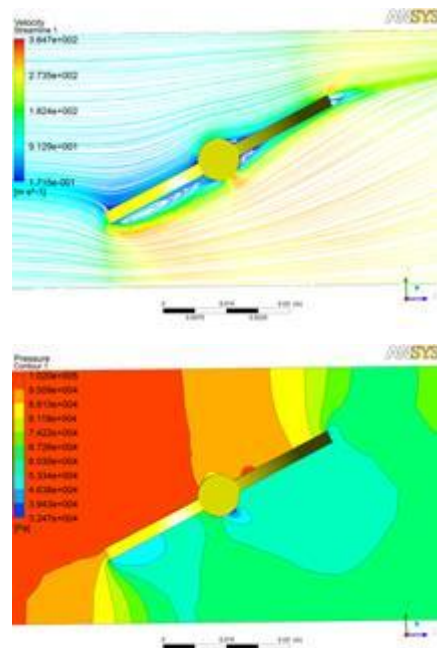


Fig. 8. Streamlines and pressure contours at  $(\theta=60^\circ)$

In addition, with the increasing of the opening angle, the flow accelerates through the pipe section past the throttle plate, and then it is divided on both sides of the latter. The streamlines becoming uniform which indicates the reduction of the flow disturbance. There is a stagnation point on the upstream side of the throttle plate where the pressure is higher due to the kinetic energy conversion (Fig. 9). For large opening angles, the flow is at near sonic velocity on both sides of the throttle valve, especially, near the throttle shaft. At large opening angles, the point of detachment is observed at the vertical diametrical plane of the throttle shaft. The lower pressure in the flow characterizes this point of separation.

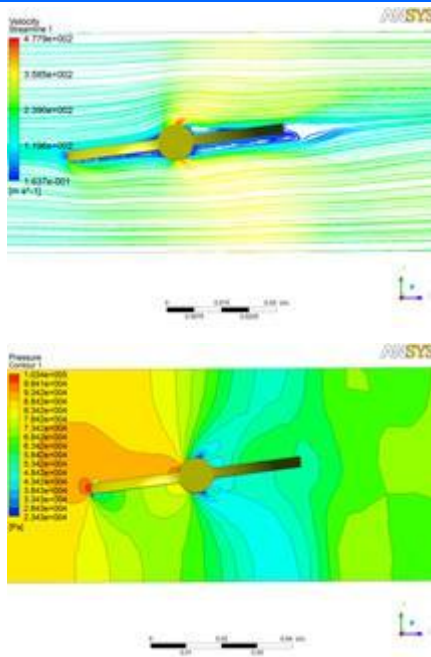


Fig. 9. Streamlines and pressure contours at ( $\theta=80^\circ$ )

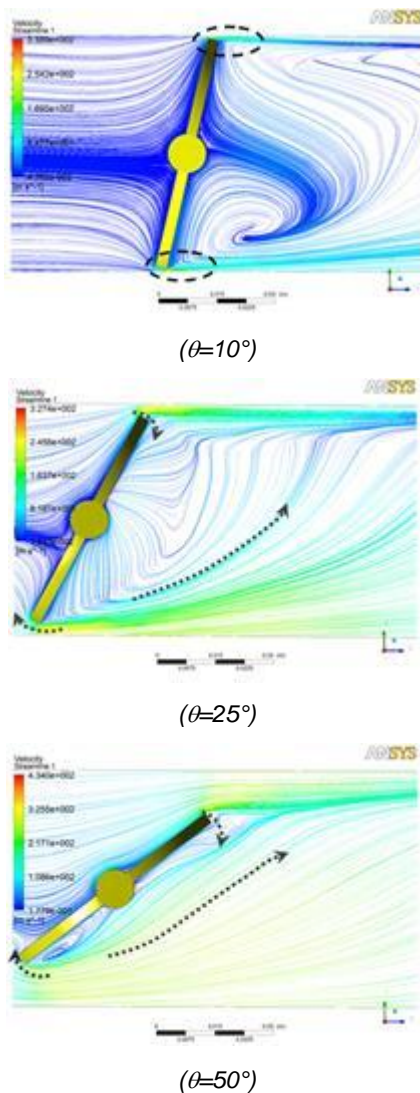


Fig. 10. Evolution of the jets issuing from valve throat

The jets on the other side of the wake (at part throttle) are at near sonic velocity. There is little or no mixing between the two jets at small angles. Hence, if an imperfect distribution of the fuel-air mixture occurs above the throttle plate (in engine manifold for the real case), it was not corrected immediately below the throttle plate. The mixing between the two jets was distinguished at large angles. Also, it is observed that, the jet in opposite direction of the valve opening always has the large spread towards the other on the same direction of the valve opening, the later keeps uniform streamlines just relative to the opening section (Fig.10,  $\theta=50^\circ$ ).

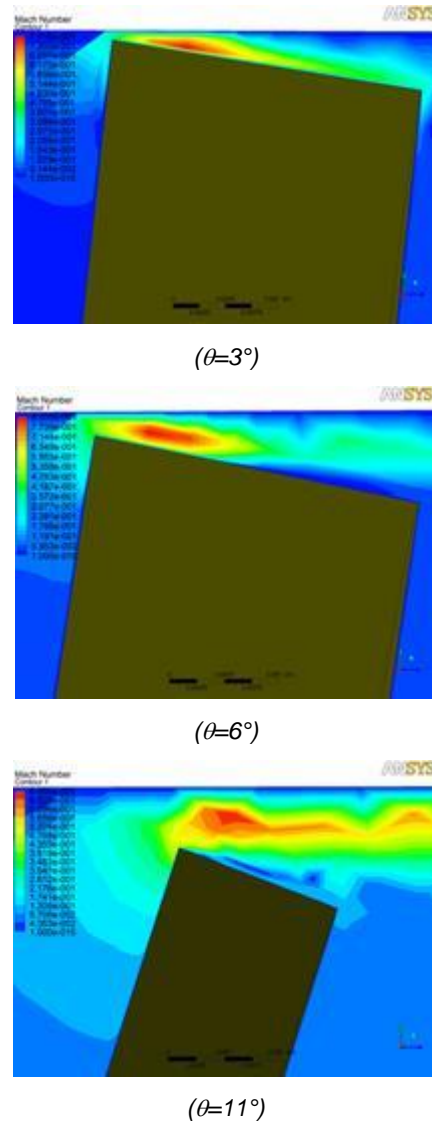


Fig. 11. Evolution of the jets issuing from valve throat

From the contours of the Mach number (Fig. 11), it is observed that the flow is at near sonic velocity around the perimeter of the throttle valve at small and intermediate opening angles. The gas flow velocity increases at the throat due to the decrease of the passage area. At the upstream of the throttle plate, the velocity is greater than that at the downstream since the temperature is identical but the pressure is lower. With the application of mass conservation principle, the gas velocity upstream of throttle plate is then

greater than the downstream. These phenomena explain the errors between real state and modeling. For small angles, it was observed that the flow is at near sonic velocity through the section of pipe near the throttle and it was at sonic velocity near the shaft of the throttle for large angles (Fig.11).

## VI. EXPERIMENTAL VALIDATION

Characterization of this kind of flow is done in both: gas stand and on-engine test bench. In our study, validation results were obtained from gas stand [9] which provides the most accurate engine-independent data by the use of Sonic Nozzle Flow Bench. The method takes one of two forms which can be interchanged to check each other:

- In the first form, throttle angle is fixed and sonic nozzles are used in combinations to give either increasing or decreasing flow.
- The second form fixes a set of sonic nozzles to set a fixed flow, then sweeps throttle angle. The second form of the method allows extremely dense data to be taken with a minimum of intervention.

The throttle is mounted using a vacuum tight seal to the flow bench. In the data presented here, the throttle was mounted without any other inlet system components. A pump creates a vacuum downstream of the nozzles. The devices used for the flow measurements are sonic nozzles because of their repeatability and insensitivity to downstream pressure. The parameters for the throttle studied [9], were nearly the same as those used for our numerical study: bore diameter,  $D=60$  mm; shaft diameter,  $d=10$  mm; throttle closed angle (Closed In Bore),  $\theta_{CIB}=7^\circ$ .

The discharge coefficient (or the mass flow rate coefficient) is used to take into account the modeling errors. It is determined experimentally (or numerically in our study). It is obtained by comparing the mass flow rate in experimental conditions and the mass flow rate calculated by equations (10) and (12). The ratio between these two values gives the discharge coefficient [23]:

$$C_D = \frac{\dot{m}_{num}}{\dot{m}_{th}} \quad (23)$$

The discharge coefficient depends greatly on throttle angle or area. To get good agreement at low throttle angles between theoretical functions (10 and 13) predictions and experimental or numerical data, it is necessary to add the effect of a throttle leak area. Effective leak area is significant compared to the main bore area for small angles. Leak flow represent a large percentage of flow at small angles, so it is beyond compare to scale theoretical predictions of main bore flow to experimental (or numerical) data without first including a leak into the throttle area calculation.

First, we can note that pressure ratios between about 0.32 and 0.90 correspond to the operational

range of frequency for an internal combustion engine [750-6000] rpm [9]. Sudden throttle angle increase may cause momentarily flows above the 6000 rpm frequency while the manifold fills. Similarly, sudden decrease will cause momentarily flows below the 750 rpm frequency while the manifold is evacuated.

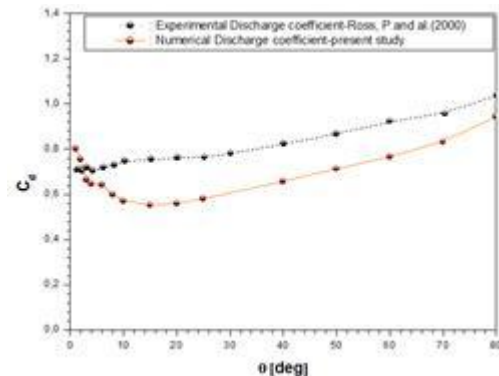


Fig. 12. Discharge coefficient

Results are presented on Fig. 12. For small angles ( $\theta = 0^\circ-10^\circ$ ), the engine is unlikely to operate in the subsonic region, it will be transiently reach outside the operational range of frequency already described. However, for these small throttle angles, a significant risk exists to a simple minded use of the  $C_D$  data. For small throttle angles,  $C_D$  data is extremely sensitive to estimated leak area. Effective leak area can vary significantly during manufacturing and tends to decrease with use due to deposits. Main bore throttle flow area is smallest at small angles so leak area effect is largest there. Since there is usually a slight leak, observed flow is larger than flow predicted with main bore area. To model main bore flow adequately, we first added leak area to the area estimated with which we normalized. We get good data fits for small angles if we only consider the sonic region.

For intermediate angles ( $\theta=10^\circ-35^\circ$ ), which correspond to strong incidences, the  $C_D$  numerical values are underestimated in comparison to the experimental values. In this range of angles, the flow detachment (separation) appears near the smallest cross section. An orifice model was appropriate at intermediate angles by a proper selection of the operational range of frequency for the internal combustion engine.

For angles from  $35^\circ$  to  $80^\circ$ , we have said that the curve of  $C_D$  for numerical data follows the same shape of the experimental one (Fig. 12) despite that the later overestimates the numerical one. For a throttle valve angle greater than  $35^\circ$ , the numerical discharge coefficient increases as the experimental one. The discharge coefficient is a function of the shape of the passage, the Reynolds number, Mach number and the gas proprieties. For a Mach number at the throat less than about 0.7, and for passages of similar shape, the discharge coefficient is essentially a function of Reynolds number only [24].

## VII. CONCLUSIONS AND RECOMMENDATIONS

Certainly, fluid or gas flow across the throttle valve of an internal combustion engine is neither isentropic nor one-dimensional. Consequently, to imitate correctly this kind of flow by the use of 1D model, other characteristics as 3D effects, must be embodied in the discharge coefficient. The aptitude to calculate this parameter ( $C_D$ ) depends on an appropriate characterization of the flow area profile as function of opening throttle angle.

Flow estimation using expressions of BSV model, will be easily affected by the small variations in pressure ratio measurements at operating regimes, such as low-speed WOT operations, where the pressure ratios tends to unity. This is the useless practical defect or failing of using this model to estimate the mass flow rate. We note that numerical results confirm that of analytical one, in which for the later, as opening valve angle increase, the pressure ratios tends to unity and the function of this ratios in the expressions of BSV model becomes very sensitive to this parameter. Consequently, the estimation of discharge coefficient for opening angle near (WOT) is not successful. Also, we remark that for intermediate angles ( $10^\circ$  to  $35^\circ$ ) which correspond to strong incidences, the mass flow rate coefficient is not influenced by the pressure ratio or the engine regime. The passage area of gas reaches a maximal value for approximately  $71^\circ$  for the opening angle of throttle plate. Beyond this angle, the shaft of the throttle plate limits the passage of gases.

Another important fact is that, the mass flow rate through the throttle valve is expressed in function of the total pressure and total temperature at the upstream side, and the ratio between downstream static pressure and the upstream total pressure. However, in real cases, the pressure measured on experimental apparatus of internal combustion engines, is the static pressure. Hence, taking into account the inlet velocity allowed important corrections in the expressions of the mass flow rate. In CFD calculations, we can use directly the total (pressure and temperature) calculated at the inlet conditions. These notions result from the application of the first principal of thermodynamics and permit to evaluate the variation of the system kinetic energy. In this situation, the hypothesis of no thermal exchange or adiabatic transformation and where, the upstream pressure is greater than the downstream pressure are considered.

Finally, we recommend that the isentropic compressible flow model (Barré de Saint Venant model), must be revised by the new corrections in the expression of mass flow rate (equations from (19) to (22)). For the same subject, an appropriate expression for the discharge coefficient must be established.

## REFERENCES

- [1] H. Hong, G.B. Parvate-Patil, B. Gordon, "Review and analysis of variable valve timing strategies - eight ways to approach", Proceedings of the Institution of Mechanical Engineers, Part D, Journal of Automobile Engineering, Volume 218, n°10, pp. 1179-1200, 2004
- [2] J.D. Anderson, "Computational Fluid Dynamics - The basics with applications", McGraw-Hill, 1976
- [3] J.I. Ramos, "Internal combustion engine modelling", Hemisphere Publishing Corporation, 1989
- [4] C. Arcoumanis, J.H. Whitelaw, "Fluid mechanics of internal combustion engines - a review", Proceedings of the Institution of Mechanical Engineers, Part C, Journal of Mechanical Engineering Science, Volume 201, n°1, pp. 57-74, 1987
- [5] D. Chalet, A. Mahé, J.F. Hetet, J. Migaud, "A new modeling approach of pressure waves at the inlet of internal combustion engines" Journal of Thermal Science, Volume 20, n°2, pp. 181-188, 2011
- [6] D. Chalet, A. Mahé, J. Migaud, J.F. Hetet, "A frequency modelling of the pressure waves in the inlet manifold of internal combustion", Applied Energy, Volume 88, n°9, pp. 2988-2994, 2011
- [7] A. Chow, M.L. Wyszynski, "Thermodynamic modelling of complete engine systems - a review", Proceedings of the Institution of Mechanical Engineers, Part D, Journal of Automobile Engineering, Volume 213, n°4, pp. 403-425, 1999
- [8] D. Chalet, P. Chesse, "Analysis of unsteady flow through a throttle valve using CFD", Engineering Applications of Computational Fluid Mechanics, Volume 4, n°3, pp. 387-395, 2010
- [9] P. Ross, A.J. Kotwicki, S. Hong, "Throttle flow characterization". SAE 2000 World Congress, 2000- 01-0571, Detroit, Michigan, 2000
- [10] M.R. Gharib, M. Moavenian, "A new generalized controller for engine in idle speed condition", Journal of Basic and Applied Scientific Research, Volume 2, n°7, pp. 6596-6604, 2012
- [11] J.J. Moskwa, "Automotive engine modeling for real time control" PhD Thesis, Massachusetts Institute of Technology, 1988
- [12] D.E. Winterbone, R.J. Pearson, "Design techniques for engine manifolds - Wave action methods for IC Engines", Professional Engineering Publishing Limited London and Bury st Edmunds, UK, 1999.
- [13] M. Bordjane, D. Chalet, M. Abidat, P. Chesse, "Inertial effects on fluid flow through manifolds of Internal Combustion Engines" Proceedings of the Institution of Mechanical Engineers, Part A, Journal of Power and Energy, Volume 225, n°6, pp. 734-747, 2011
- [14] D.E. Winterbone, R.J. Pearson, "Theory of engine manifold design - Wave action method for IC Engines, Professional Engineering Publishing Limited London and Bury st Edmunds, UK, 2000.

- [15] D.C. Wilcox, "Turbulence modeling for CFD", DCW Industries, 2006
- [16] J. Tu, G.H. Yeoh, C. Liu, "Computational Fluid Dynamics: a practical approach", Butterworth-Heinemann, 2012
- [17] B.E. Launder, D.B. Spalding, "The numerical computation of turbulent flows", Computer Methods in Applied Mechanics and Engineering, Volume 3, n°2, pp. 269-289, 1974
- [18] H. Cho, H. Song, J. Lee, S. Kauh, "Simulation of a transient torque response for engine performance in a spark ignition engine", Proceedings of the Institution of Mechanical Engineers, Part D, Journal of Automobile Engineering, Volume 215, n°1, pp. 127-140, 2001
- [19] C.F. Taylor, "The internal combustion engine in theory and practice", Volume 1, The MIT Press, 1985
- [20] S. Thompson, S.Y. Duan, "Modelling parameter selection and simulation of a single-cylinder four-cycle engine". Proceedings of the Institution of Mechanical Engineers, Part I, Journal of Systems and Control Engineering, Volume 205, n°1, pp. 49-57, 1991
- [21] M. Cary, M. Ebrahimi, K. Ffrench, R. Sbaschnig, "Throttle body: modelling and identification", Proceedings of the Institution of Mechanical Engineers, Part D, Journal of Automobile Engineering, Volume 215, n°7, pp. 813-825, 2001
- [22] D.L. Harington, J.A. Bolt, "Analysis and digital simulation of carburetor metering", SAE Technical Paper 700082, 1970
- [23] P. Giansetti, "Contrôle moteur à allumage commandé. Estimation/prédiction de la masse et de la composition du mélange enfermé dans le cylindre", PhD Thesis, Université d'Orléans, 2005
- [24] J.B. Heywood, "Internal Combustion Engine Fundamentals", McGraw-Hill, 1988

## NOMENCLATURE / SYMBOLS

$A_{\text{bore}}$	Throttle body bore area [m <sup>2</sup> ]
$A_e$	Effective area [m <sup>2</sup> ]
$A(\theta)$	Throttle plate open area [m <sup>2</sup> ]
$C_D$	Discharge coefficient
$C_p$	specific heat of air at constant pressure [KJ/kg.K]
$C_\mu$	k- $\varepsilon$ turbulence model constant
$C_{\varepsilon_1}$	k- $\varepsilon$ turbulence model constant
$C_{\varepsilon_2}$	k- $\varepsilon$ turbulence model constant
$D$	Bore diameter of throttle body [m]
$d$	Shaft diameter of the throttle plate [m]
$k$	Turbulence kinetic energy [m <sup>2</sup> /s <sup>2</sup> ]

$\dot{m}$	Air mass flow rate [kg/s]
$p_m$	Intake manifold pressure [Pa]
$p_0$	Ambient pressure [Pa]
$p'$	Modified pressure [Pa]
$R_{sa}$	Specific gas constant of air =287 [KJ/kg.K]
$T_0$	Ambient temperature [K]
$U_j$	Velocity components [m/s]
$x_j$	Cartesian coordinates in x, y and z directions [m]

## Greek letters

$\gamma$	Specific heat ratio (=1.40)
$\varepsilon$	Turbulence kinetic energy dissipation [m <sup>2</sup> /s <sup>3</sup> ]
$\theta$	Throttle plate opening angle [deg]
$\theta_0$	Throttle plate angle at closed position [deg]
$\mu$	Molecular (dynamic) viscosity [kg/m.s]
$\mu_t$	Turbulent viscosity [kg/m.s]
$\rho$	Fluid density [kg/m <sup>3</sup> ]
$\sigma_k$	k- $\varepsilon$ turbulence model constant
$\sigma_\varepsilon$	k- $\varepsilon$ turbulence model constant

## Subscripts

init	initial
num	numerical
th	theoretical
do	downstream
up	upstream
stat	static
tot	total
dyn	dynamic
CIB	Closed In Bore

## Abbreviations

BSV	Barre de Saint Venant
AFR	Air-Fuel Ratio
WOT	Wide Open Throttle
rpm	revolution per minute